

CURVE SQUEAL OF TRAIN WHEELS: UNSTABLE MODES AND LIMIT CYCLES

PACS REFERENCE: 43.40Dx

Heckl, Maria
Department of Mathematics
Keele University
Staffordshire ST5 5BG
United Kingdom
Tel: +44 1782 583423
Fax: +44 1782 584268
e-mail: m.a.heckl@maths.keele.ac.uk

ABSTRACT

When a train goes round a curve, a transverse friction force may act between the wheels and the rail in such a way that the wheels are excited to perform bending oscillations and to radiate squeal noise. This phenomenon has been modelled theoretically and simulated numerically. Each wheel is described by a superposition of bending modes. It is excited transversely by a stick/slip friction force, which depends nonlinearly on the wheel velocity. The growth rates of individual wheel modes are calculated, revealing the linearly unstable modes. The time history of the oscillation is also calculated, revealing the modes that form the limit cycle.

INTRODUCTION

Curve squeal of trains is generated if a train traversing a bend performs a crabbing motion with its wheels because they cannot align themselves tangentially to the rail. As a consequence of this crabbing motion, a dry friction force acts laterally at the wheel/rail contact. The friction force excites bending oscillations of the wheels, and the wheels then radiate sound into the surrounding air. The frequency spectrum of the squeal sound contains one (or a few) sharp peaks, and each peak corresponds to the resonance of a certain bending mode of the wheels.

Curve squeal is an example of a friction-driven oscillation, where the friction force oscillates in rapid succession between sliding friction (slip) and sticking friction, giving rise to a limit cycle of stick/slip oscillation. The aim of this paper is to shed some light on the criteria by which a particular mode (or set of modes) is selected for the limit cycle of a given wheel.

THE GOVERNING EQUATIONS

The free wheel is assumed to be a linear system, therefore the transverse displacement w of the friction-driven wheel (see Heckl and Abrahams 2000) is given by

$$w(r, \varphi, t) = \int_{t'=0}^t F(v(r', \varphi', t')) G(r, \varphi; r', \varphi'; t - t') dt' . \quad (1)$$

(r, φ) is an observer point on the wheel and (r', φ') is the contact point with the rail where the friction force acts. t is the observer time and t' are all the moments in time at which the friction force acts on the wheel. v is the wheel velocity and $F(v)$ is the friction characteristic. G , the Green's function, is the displacement response of the free wheel to an impulse point force acting at (r', φ') .

The friction characteristic $F(v)$ describes the feedback between the wheel oscillation and the friction force driving this oscillation. $F(v)$ is assumed to be the piecewise linear function given by

$$F(v) = \begin{cases} F_0 + \gamma v & \text{for } v < v_c \text{ and } v > V + \Delta V \text{ (slip)} \\ \Gamma(v - V) & \text{for } v \in (v_c, V + \Delta V) \text{ (stick).} \end{cases} \quad (2a,b)$$

γ denotes the (positive) slope of the slip section; it can be seen as a "negative damping coefficient" associated with sliding friction. Γ is the (negative) slope of the stick section. F_0 is the value of the friction force where $v = 0$; in physical terms it is a measure of the normal force (due to the weight of the wheel and/or train) that acts on the contact point. V is the value of the wheel velocity where $F = 0$; in physical terms it is the crabbing speed. The critical velocity v_c , where the change-over from slip to stick occurs, is given by $v_c = (F_0 + \Gamma V)/(\Gamma - \gamma)$. ΔV , given by $\Delta V = (\gamma V + F_0)/(\gamma - \Gamma)$, is a measure of the narrow velocity interval that encloses the stick section of the friction characteristic. The friction characteristic given in (2) is a piecewise linear approximation of a typical measured curve. It is also close to the friction characteristic used in

early models of the bowed violin string (McIntyre and Woodhouse 1979). The bow speed and normal force due to pressure on the bow correspond respectively to the crabbing speed V and the normal force F_0 .

The Green's function characterises the *free* wheel, i.e. the wheel that is merely held by the axle without making contact with the rail. It is a superposition of the bending modes of the wheel,

$$G(r, \varphi; r', \varphi'; t - t') = \begin{cases} \operatorname{Re} \sum_{m=0}^{\infty} \sum_{n=1}^{\infty} g_{mn}(r, \varphi; r', \varphi') e^{-i\omega_{mn}(1-i\eta_{mn})(t-t')} & \text{for } t \geq t' \\ 0 & \text{for } t < t'. \end{cases} \quad (3a,b)$$

ω_{mn} , η_{mn} and g_{mn} are respectively the frequency, loss factor and amplitude of mode (m,n) . The integers m and n denote the number of nodal lines and nodal circles, respectively. The Green's function components can be determined experimentally by exciting the free wheel with an impulse point force and then measuring the time history of the resulting motion. The frequency, loss factor and amplitude of each mode are then inferred from the measured time history. The loss factors are assumed to include any relevant damping mechanisms, such as radiation losses and various forms of internal damping. This experimental approach is possible for wheels of any geometry. For wheels of simple geometries, the frequencies and amplitudes of the Green's function can be calculated theoretically.

If equation (1) is combined with (3) and evaluated at $(r, \varphi) = (r', \varphi')$, one obtains the governing equation for the wheel motion at the contact point. This can be solved analytically as an eigenvalue problem for the special case of a purely linear friction characteristic, given by $F(v) = F_0 + \gamma v$ for the whole velocity range; this gives the modal frequencies and growth rates Δ_{mn} (Heckl 2000), and also the time t_{mn} it takes an unstable mode (m,n) to reach the critical velocity v_c . If the friction characteristic is nonlinear, as given in (2), the governing equation can only be solved numerically; this gives the time histories of wheel velocity and friction force.

NUMERICAL RESULTS

Numerical simulations were performed for a friction characteristic given by equations (2a,b) with $\gamma = 15\,000\text{ Ns/m}$ (slope of the slip section), $\Gamma = -100\,000\text{ Ns/m}$ (slope of the stick section), $V = 50 \times 10^{-6}\text{ m/s}$ (crabbing speed), $F_0 = 1.07\text{ N}$ (measure of normal force). This gives $v_c = 34.2 \times 10^{-6}\text{ m/s}$ for the critical velocity, where the oscillation changes from slip-only to stick/slip.

The wheel used in the simulations is a model wheel, made from steel; it has the shape of a flat circular disc with a hub at the centre and has measurements $d = 0.003\text{ m}$ (wheel thickness), $a = 0.038\text{ m}$ (wheel radius), $b = 0.010\text{ m}$ (hub radius). Its eigenfrequencies ω_{mn} , Green's function amplitudes g_{mn} (which are pure imaginary), and loss factors η_{mn} are listed in Table 1.

(m,n)	$\omega_{mn} [2\pi\text{ s}^{-1}]$	$\text{Im}(g_{mn}) [10^{-9}\text{ m/Ns}]$	η_{mn}
(0,1)	3020	1969	0.07
(1,1)	2922	4124	0.07
(2,1)	3655	3472	varied
(3,1)	6482	2141	varied
(4,1)	10980	1409	varied

Table 1 Properties of the free wheel

The mode pair (2,1)/(4,1) is nearly harmonically related, $\omega_{41} \approx 3\omega_{21}$, but none of the other mode pairs are. Only the first five modes ($m = 0, \dots, 4, n = 1$) have eigenfrequencies within the range of audible frequencies, and only those modes are included in the numerical simulations presented here. They all have just one nodal circle, which coincides with the edge of the wheel hub.

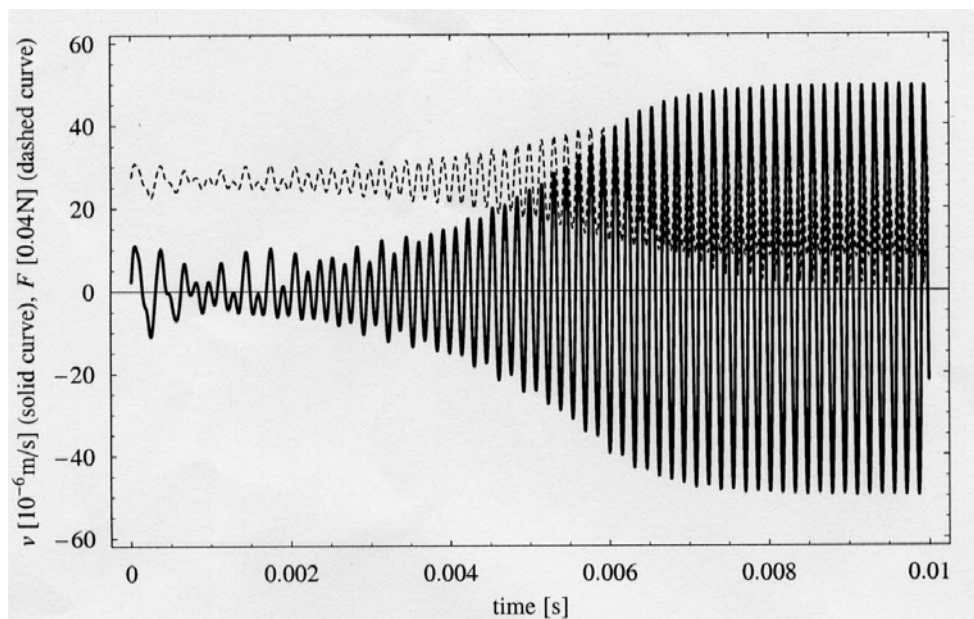
The numerical simulations focus on the three modes (2,1), (3,1) and (4,1) and investigate their interplay under nonlinear conditions. Their modal loss factors are varied in order to simulate different degrees of instability. The other two modes have a high loss factor and are stable throughout ($\Delta_{01} \approx -1200\text{ s}^{-1}$, $\Delta_{11} \approx -600\text{ s}^{-1}$). The simulation results for four representative cases are listed in Table 2.

η_{21}	η_{31}	η_{41}	$\Delta_{21} [s^{-1}]$	$\Delta_{31} [s^{-1}]$	$\Delta_{41} [s^{-1}]$	$t_{21} [10^{-3} s]$	$t_{31} [10^{-3} s]$	$t_{41} [10^{-3} s]$
0.0400	0.0040	0.0400	-304	494	-203	-	5.44	-
0.0400	0.0040	0.0050	-304	493	381	-	5.45	8.19
0.0400	0.0040	0.0018	-304	493	602	-	5.45	5.18
0.0100	0.0400	0.0100	403	-978	37	5.09	-	83.87

Table 2 Loss factors η , linear growth rates Δ and growth times t of cases 1 to 4

One Unstable Mode (Case 1 in Table 2)

The time history corresponding to case 1, where mode (3,1) is unstable ($\Delta_{13} > 0$) is shown in the figure below.



Many more time histories have been calculated for other wheels with one mode, say mode (m,n) , unstable on its own. These time histories share the same features: initially, there is an exponential amplitude growth with rate Δ_{mn} , then there is a slower growth followed by a limit cycle with the frequency ω_{mn} and limit cycle amplitude V (crabbing speed).

Two Unstable Modes, Not Harmonically Related (Cases 2 and 3 in Table 2)

The time histories (not illustrated) show that in case 2 ($t_{31} < t_{41}$), mode (3,1) forms the limit cycle, and in case 3 ($t_{41} < t_{31}$), mode (4,1) forms the limit cycle. Many more simulations have been made, and they show that if there are two unstable modes that are not harmonically related, the limit cycle will be formed by one of them. The crucial factor that selects this mode is the time it takes for the velocity of this mode to reach the critical value where the friction force

becomes nonlinear. The situation is very much like a race between the unstable modes competing for the limit cycle, which is won by the mode that reaches the critical value in the shortest time. A high linear growth rate and a large Green's function amplitude are the features that allow a short growth time. The limit cycle establishes quickly if there is a big difference between the growth times; if the two growth times are quite similar, the transition into the limit cycle is not smooth, and may take a long time.

Two Unstable Modes, Harmonically Related (Case 4 in Table 2)

The two modes (2,1) and (4,1) are harmonically related ($\omega_{41} \approx 3\omega_{21}$). This allows their coexistence in the limit cycle (not illustrated). Two such modes can coexist in the limit cycle with the lower mode dominating, but not with the higher mode dominating. The presence of the higher mode in the limit cycle is most pronounced if the frequency ratio is 2:1, and it becomes less pronounced with increasing frequency ratio. The modes have to be exactly or very nearly harmonically related in order to coexist in the limit cycle. If the deviation between the actual frequency of the higher mode and the exact harmonic is more than $\pm 5\%$, coexistence is not possible.

CONCLUSIONS

This paper has examined curve squeal by modelling a wheel driven by a piece-wise linear friction characteristic, which is typical for stick/slip oscillations.

Curve squeal can be eliminated if the unstable amplitude growth can be prevented. This has been achieved in practice by increasing the wheel damping (equivalent to increasing the modal loss factors in our model). It has also been achieved by applying lubrication to change the properties of the wheel/rail interface in such a way that the slope of the increasing section of the friction characteristic is lessened (equivalent to changing the friction characteristic in our model in such a way that the gradient of the slip section is reduced). Curve squeal can be reduced in intensity by reducing the train speed and by increasing the curve radius; both measures reduce the crabbing speed which, according to our model, determines the velocity maximum of the limit cycle.

REFERENCES

Heckl, Maria A. and Abrahams, I.D. 2000 Curve squeal of train wheels, part 1: Mathematical model for its generation. *Journal of Sound and Vibration*, **229**, 669-693.

Heckl, Maria A. 2000 Curve squeal of train wheels, part 2: Which wheel modes are prone to squeal? *Journal of Sound and Vibration*, **229**, 695-707.

McIntyre, M.E. and Woodhouse, J. 1979 On the fundamentals of bowed-string dynamics. *Acustica*, **43**, 93-108.